

Fibre reinforced polymer strengthening of the Sainte-Émélie-de-l'Énergie bridge: design, instrumentation, and field testing

P. Labossière, K.W. Neale, P. Rochette, M. Demers, P. Lamothe, P. Lapierre, and G. Desgagné

Abstract: An experimental research project was undertaken to evaluate the need to strengthen existing reinforced concrete bridges belonging to the Ministère des Transports du Québec. A typical bridge consisting of a single-span bridge with T-shaped sections was identified. Evaluation of the bridge showed that an increase in bending strength and shear strength would be necessary to satisfy current loading conditions and code requirements. The increase in bending strength was obtained by bonding carbon-reinforced composite materials to the underface of the beams, with fibres in the longitudinal direction. External U-shaped stirrups made of glass-reinforced composite materials were installed on the outside faces of the beams in order to increase their shear strength. This paper presents a selection of experimental results initially obtained on T-section beams, scaled 1:3 with respect to the bridge under consideration. The actual reinforcement scheme selected for the bridge is then presented, accompanied by comments on the construction process. Conventional instrumentation and fibre optic sensors were incorporated to the repair work in order to evaluate the behaviour of the bridge, before and after strengthening. Initial results of this ongoing evaluation are presented here.

Key words: bridge strengthening, FRP, composite materials, instrumentation, field testing.

Résumé : Un projet de recherche expérimental a été entrepris afin d'évaluer les techniques de renforcement des ponts appartenant au Ministère des Transports du Québec. Un pont type en béton armé a été identifié: il consiste en une seule portée avec des poutres parallèles et dalle participante. Une évaluation de l'état de ce pont typique a montré qu'une augmentation de sa résistance en flexion et aux efforts tranchants serait nécessaire afin de satisfaire aux prescriptions de la norme actuelle. L'augmentation de résistance en flexion a été atteinte par l'ajout de bandes de fibres de carbone sur la face inférieure des poutres du pont; des étriers externes en forme de U, en fibres de verre, ont permis d'augmenter sa résistance aux efforts tranchants. On trouvera dans cet article une sélection de résultats expérimentaux sur des poutres à une échelle 1:3 du pont considéré, testées en laboratoire. On présente ensuite le renforcement sélectionné pour le pont, de même que quelques résultats obtenus grâce à l'instrumentation incorporée à l'ouvrage.

Mots clés : renforcement de ponts, matériaux composites, instrumentation, application en chantier.

1. Introduction

Many countries around the world have tremendous needs to repair and strengthen their existing infrastructure. Everywhere, traffic loads have often reached levels largely exceeding the original design expectations. In addition, northern countries experience severe winter conditions leading to an

extensive use of de-icing salts. These effects combine together to cause serious deterioration in a large number of existing bridges. In recent years, fibre reinforced polymer products (FRPs) have become increasingly popular for the rehabilitation and strengthening of such structures and have generated a developing research interest (Japan Concrete Institute 1997; Meier and Betti 1997). In Canada, the extent of deterioration has prompted many authorities, including the federal and a number of provincial governments, to investigate the potential use of FRPs to extend the life of their infrastructure (Rizkalla and Labossière 1999). Typical applications of FRPs in Quebec have included major rehabilitation schemes such as the Webster Parkade in Sherbrooke and many small-scale projects such as the wrapping of reinforced concrete columns of a highway overpass by the Ministère des Transports du Québec (MTQ) at St-Étienne-de-Bolton (Neale and Labossière 1998). In many cases, the authorities have first used FRPs on projects where the structural component of the repair would not be critical but would nevertheless provide useful information on the

Received August 11, 1999.

Revised manuscript accepted February 29, 2000.

P. Labossière,¹ K.W. Neale, P. Rochette, M. Demers, P. Lamothe, and P. Lapierre. Département de génie civil, Université de Sherbrooke, Sherbrooke, QC J1K 2R1, Canada.
G. Desgagné. Direction des structures, Ministère des transports du Québec, Québec, QC G1S 4X9, Canada.

Written discussion of this article is welcomed and will be received by the Editor until February 28, 2001.

¹Author to whom all correspondence should be addressed (e-mail: pierre.labossiere@sca.usherb.ca).

durability of the composites. For instance, the lack of apparent degradation on nonstructural repair situations has led the MTQ to consider the use of FRPs for strengthening applications. The reinforced concrete structures owned by the MTQ that could now be considered for this type of strengthening should be in good structural condition and exhibit a concrete surface of good quality. The primary reason for adding strength to them is the significant increase in traffic load since their construction and increasingly stringent design codes.

This paper presents a bridge strengthening case that was completed recently in Sainte-Émélie-de-l'Énergie, where the reinforced concrete beams of a one-span bridge were reinforced using FRPs. This full-scale application was undertaken by the MTQ, following an extensive testing program at the Université de Sherbrooke. After a brief discussion of the evaluation policy of the MTQ, the most significant testing results of the 1:3 scale beams representing the target bridge are presented. The configuration of the selected reinforcement for the actual bridge is then introduced, followed by a description of the repair work. The permanent instrumentation incorporated into the bridge is briefly described, and the paper concludes with a presentation of results obtained to date.

2. Design philosophy

The condition of bridges under the jurisdiction of the MTQ is characterized by the live load rating factor LLRF, which is defined in Standard CAN/CSA-S6-88 "Design of highway bridges" (CSA 1988) as follows:

$$[1] \quad \text{LLRF} = \frac{U\phi R - \Sigma\alpha_D D}{\alpha_L L(1+I)}$$

In this equation, R is the nominal resistance of the structural element considered, and D and L are the nominal force effects due to the dead and static traffic loads, respectively. The dynamic effects of the live loads and impact are expressed as a fraction of the nominal static live loads using the factor I ($0.2 \leq I \leq 0.4$). Statistical variations in the load and material strength are taken into account with the combination of a resistance factor ϕ and load factors α_L and α_D . The equation also contains an adjustment factor U ; its value is based on the actual evaluation of the state of the bridge. Tables in the CAN/CSA-S6-88 standard provide recommended values for this parameter.

In Quebec, the live load for a bridge is usually calculated using a four-axle truck of 660 kN identified as QS-660 (Ministère des Transports du Québec 1994). When this loading condition can be sustained, the live load rating factor LLRF is found to exceed 1.0. For lower values, the current MTQ policy is the following:

- For $0.85 < \text{LLRF} < 1$, an appropriate posting signals that the bridge is forbidden to overweight trucks. Exceptionally, a reinforcement of the bridge can be undertaken to bring its capacity to the current standard level.
- For $\text{LLRF} < 0.85$, a reduced limit load is posted and enforced. However, in this case, reinforcement of the structure is generally given high priority to bring the capacity to the current standard level. Alternatively, it

Table 1. Condition of MTQ reinforced concrete beam bridges.

LLRF	Number of bridges	Average age
Not evaluated	986	39
>1	198	46
0.85–1.0	105	51
<0.85	223	52
Total	1512	42

can be recommended that the bridge be replaced by a newer structure.

It has generally been observed that the appearance and general state of the bridge are directly related to the loading capacity factor. Then, for a bridge in good condition, the LLRF is high; and for a bridge showing serious degradation, the LLRF is low. When reinforcement is the selected option, for any LLRF value, the MTQ requires that the engineers apply the same standards as for the construction of a new structure.

A recent survey of the condition of reinforced concrete beam bridges under the jurisdiction of the MTQ appears in Table 1. The priority of the MTQ is currently the reinforcement or replacement of bridges with a LLRF factor inferior to 0.85.

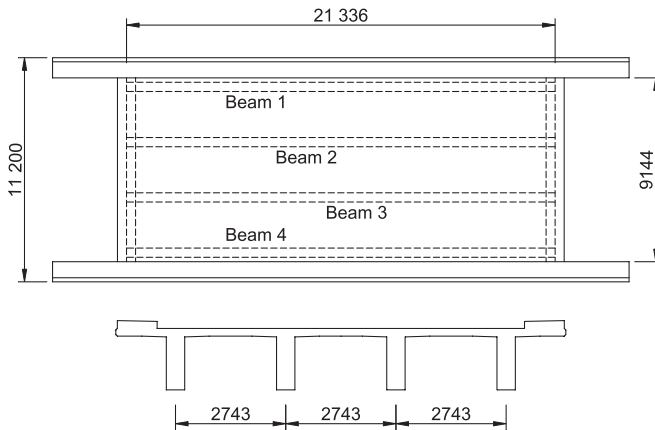
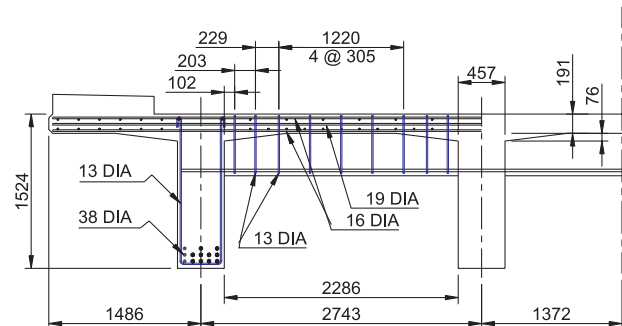
3. Bridge selection

The selection of a bridge appropriate for experimental application of composites was carried out by the MTQ. The objectives consisted of identifying a bridge with $\text{LLRF} < 1$, and for which the conditions of the materials would be good enough to facilitate the installation of composites without too much surface preparation. However, since it would be the first bridge owned by the MTQ to be reinforced in bending with FRPs, it was preferred that $\text{LLRF} > 0.85$. The bridge should be representative of the bridges on the Quebec road system.

A bridge over Rivière Noire on route 131 near the village of Sainte-Émélie-de-l'Énergie in the Laurentides-Lanaudière region, approximately 130 km northeast of Montréal, satisfied these conditions. This bridge, shown in Fig. 1, is a typical one-span river crossing on a secondary road. Although the traffic level on this road is not excessive, the bridge must sustain heavy loads induced by large timber-carrying trucks. A capacity factor LLRF of 0.94 was calculated for the bridge, and according to MTQ policies, its replacement would not be considered. However, upgrading the load-carrying capacity to the current standards was necessary to avoid the hindrance that limiting truckloads on this road would cause to the local industry.

4. Bridge characteristics

The Sainte-Émélie bridge was originally built in 1951, and the traffic load at that time was calculated using a standard 20 ton truck with the load applied through two axles, identified as H20. This is a one-span bridge of 21.3 m in length, with four parallel reinforced concrete beams and a

Fig. 1. View of the Sainte-Émélie bridge.**Fig. 2.** General features of the Sainte-Émélie bridge.**Fig. 3.** Section of the Sainte-Émélie bridge.

participating slab forming T-sections. The total width of the bridge is 11.1 m, and the traffic lanes occupy a width of 9.1 m. The general bridge configuration is given in Fig. 2. The rectangular sections below the slab are rather elongated, and there was a lack of experimental data in the literature for the FRP reinforcement of beams with those proportions. A partial section of the bridge as it appears in the original drawings, showing steel reinforcement details, is presented in Fig. 3.

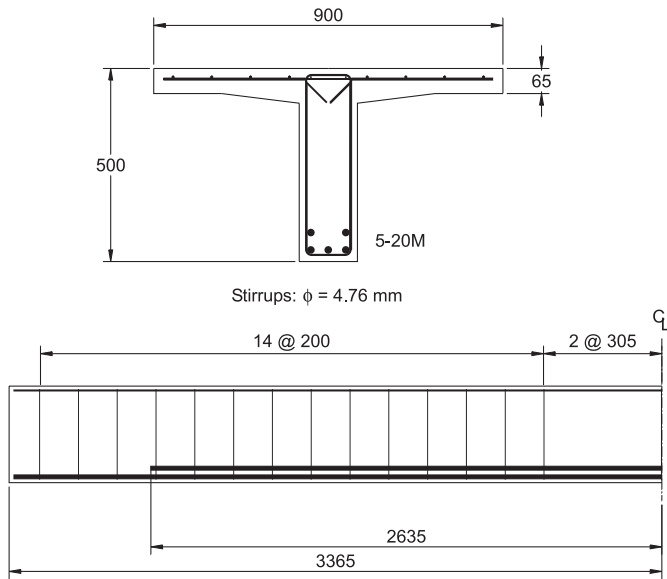
Using the S6-88 standard and truck load QS-660, it was found that the flexural strength would have to be raised by 35%, while the shear strength would have to be increased by 20%. These levels of additional reinforcement, and the general condition of the bridge, for which there was neither significant spalling of concrete nor degradation of steel rebar through corrosion, made this bridge appropriate for full-scale experimentation.

5. Laboratory testing

Prior to the reinforcement of the actual bridge, the Ministère des Transports sponsored a research project at the Université de Sherbrooke to evaluate the potential for FRP strengthening. This project comprised laboratory studies on scaled specimens and numerical modelling of the repair schemes considered. The extensive laboratory testing program included mechanical tests on different FRP products, the evaluation of a variety of strengthening configurations in shear and bending for rectangular and T-section beams, testing of the FRP bonding capacity to the concrete surface, and evaluation of potential climatic effects on FRP-strengthened structural elements. Only details of the tests performed on T-beams are presented here (Lamothe et al. 1998; Lapiere et al. 1998; Labossière et al. 1998).

The sections of the four reinforced concrete T-beams tested in the laboratory are shown in Fig. 4. The internal reinforcement of the 6500-mm-long beams consists of five 20M rebars, and the shape and geometry of the section were

Fig. 4. Section of T-beams for testing program.



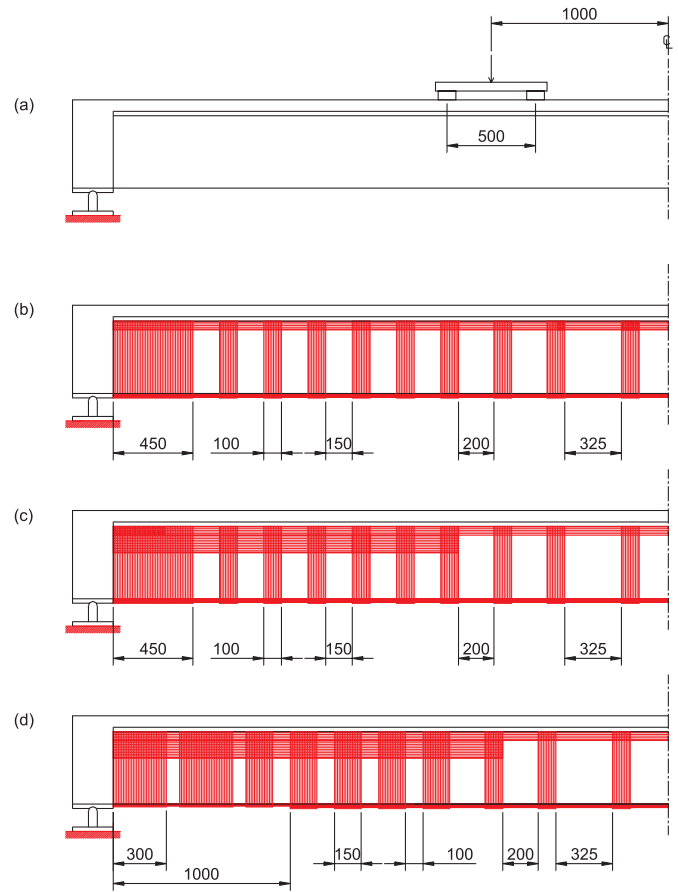
determined in order to reproduce as accurately as possible the behaviour of the Sainte-Émélie bridge, on an approximately 1:3 scale. The figure indicates the position of the shear reinforcement and of the steel mesh in the slab. Loading was applied with two actuators, spaced 2000 mm from each other, in the centre of the beam. The load from each actuator was further divided in two points spaced 500 mm c/c. For this combination of loading and reinforcement, bending and shear failures were expected to occur simultaneously. The configurations of the composite reinforcement schemes studied to increase the capacity of the T-beam are shown in Fig. 5.

The beams are identified as follows:

- T1: reference beam, with no FRP reinforcement;
- T2: beam reinforced in bending on the full length with six 83-mm-wide layers of *Replark-20*, and in shear with 100-mm-wide U-shaped *Fibrwrap* stirrups, generally alternating with 150-mm free space. Anchorage of the stirrups is improved through an additional 50-mm-wide longitudinal *Fibrwrap* band on the full length of the beam.
- T3: beam reinforced in bending with one 50-mm-wide *Carbodur S* plate on the full length of the beam, and U-shaped *Fibrwrap* external stirrups. The stirrup spacing is the same as for beam T2. However, a wider anchoring band was installed on top of the stirrups, near the slab.
- T4: beam reinforced in bending with six 83-mm-wide layers of *Replark-20*. Three of these layers extend on the full length of the beams, while the three remaining layers are 1 m shorter at both ends, thus allowing savings of about 16% of material without significant changes in bending strength. While the total fibre quantity in bending is the lowest of the three strengthened T-beams, Fig. 5 shows that a higher area of external stirrups was used near the extremities.

Material properties considered for modelling of the beams are given in Table 2. Concrete and steel rebars properties were measured in the laboratory, and the FRP values given

Fig. 5. FRP reinforcement for laboratory testing: (a) T1, reference; (b) T2, *Replark 6s.*; (c) T3, *Carbodur 1p.*; (d) T4, *Replark 6s./3s.* optimized.

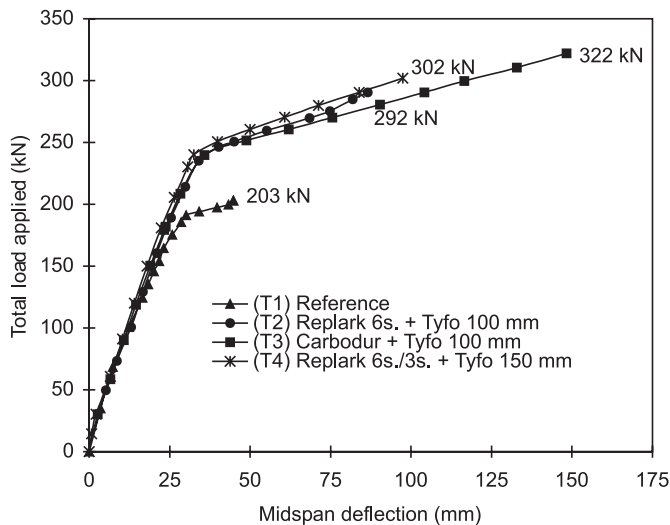


in the table are those appearing at the time on technical data sheets provided by the manufacturers of these products. Our own coupon testing of these products confirmed that these values could be used safely for design purposes. The experimental load–deflection curves for the four T-beams are shown in Fig. 6. Photographs of the characteristic failure modes are presented in Fig. 7. The following are some general observations about the beam behaviour.

For the reference beam, failure was expected to occur simultaneously in shear and bending under the applied loads. Shear cracks oriented at 45° near the supports appeared early in the loading of beam T1. The beam failed in shear; however, at that point yielding of the lower steel rebars had already been measured. Figure 7a shows the width of shear cracks at failure near the support. Beam T2, also failed in shear, was able to sustain a total load 40% higher than T1. Failure was initiated by debonding of an external composite stirrup. Figure 7b shows the failure area near the support, where the shear crack is visible through the FRP stirrups and extends up into the slab. This test demonstrated that the 50-mm-wide longitudinal anchoring band was not sufficient to transfer the shear stresses to the concrete and was therefore widened for beams T3 and T4. This increased anchorage proved to be sufficient for T3; the beam sustained a load 60% higher than T1. The loading test was interrupted when the *Carbodur S* longitudinal strengthening failed in tension.

Table 2. Material properties for laboratory T-beams.

Material	Property
Concrete	$f'_c = 47$ MPa
Steel rebars #15M	$f_y = 430$ MPa $f_u = 620$ MPa $\epsilon_y = 0.2\%$ $\epsilon_{sh} = 0.9\%$ $\epsilon_u = 15\%$
Steel stirrups $\phi = 4.76$ mm	$f_y = 600$ MPa $f_u = 680$ MPa $\epsilon_y = 0.3\%$ $\epsilon_{sh} = 0.3\%$ $\epsilon_u = 5\%$
Carbodur-S (Sika)	Carbon fibres Thickness = 1.2 mm/ layer $f_u = 2400$ MPa $\epsilon_u = 0.0155\%$ $E = 155$ GPa Fibres volume = 68%
Replark-20 (Mitsubishi)	Carbon fibres Thickness = 0.11 mm/ layer $f_u = 3400$ MPa $\epsilon_u = 0.0148\%$ $E = 230$ GPa Fibres volume = 100%
SEH51-Tyfo (Hexcel-Fyfe)	Glass fibres Thickness = 1.3 mm/ layer $f_u = 454$ MPa 0.02 $E = 22.7$ GPa Fibres volume = 25%

Fig. 6. Load–deflection curves for the 1:3 scale T-beams.

Many signs of damage in the composite stirrups and on the concrete surface had been observed in the beam before failure. The longitudinal *Replark-20* reinforcement of beam T4, which had been optimized by reducing it by half near the end supports, was also the first to fail. The total applied load at failure was 50% higher than the one sustained by the reference beam. Figure 7c shows the large deflection observed before failure.

An important observation from the T-beams reinforced with composites was that the deflection at failure always exceeded that measured for the reference beam. The initial stiffness of the beam did not appear to be significantly modified by the additional reinforcement. Yielding of the rebars was observed prior to the failure of the three FRP-reinforced beams. There were also similar concrete deformations in the three beams at similar load levels. The two carbon-reinforced products used to improve the bending strength of the beams behaved in almost the same way; the selection of one over another would clearly be a matter of selecting the most appropriate installation procedure for a given application.

In general, the above tests confirmed the potential for reinforcing T-beams with carbon fibre composite materials. The load–deflection curves were consistent with models that were being developed at the time. They also provided useful information on the selection of the external stirrups that should also be installed on these beams to improve their shear strength.

6. Bridge reinforcement

6.1. Calculation methods

The behaviour of the beams tested in the laboratory confirmed some design assumptions, which were subsequently used to design the actual bridge reinforcement. These assumptions are (i) plane sections remain plane; (ii) bond between concrete, steel, and composite is perfect; (iii) shear strains can be neglected; and (iv) a proper anchorage is ensured to prevent premature debonding of the FRP.

The method of analysis is based on the same assumptions as those in CSA Standard S6 for reinforced concrete bridges. The parabolic distribution of stresses in concrete above the neutral axis is replaced by an equivalent rectangular distribution of height a and uniform stress $\alpha_1 f'_c$, with

$$[2] \quad \alpha_1 = 0.85$$

and

$$[3] \quad a = \beta_1 c$$

$$[4] \quad 0.85 \geq \beta_1 = 1.09 - 0.008 f'_c \geq 0.65$$

where c is the position of the neutral axis measured from the top of the beam.

In bending, failure may occur in one of the following modes, depending on the combination of section dimensions and material properties: (i) concrete crushing; (ii) steel yielding followed by concrete crushing; (iii) steel yielding followed by FRP rupture; and (iv) debonding of the FRP reinforcement.

Using the equilibrium equation of the section, and assuming linear relationships between internal strains, the position c of the neutral axis can be computed using the following:

$$[5] \quad \phi_c \alpha_1 f'_c \beta_1 b c = \phi_s f_y A_s + \phi_{frp} E_{frp} A_{frp} \varepsilon_{frp}$$

where ε_{frp} is the strain in the composite when the beam fails. The value of ε_{frp} depends on the failure mode. Since this failure mode is unknown a priori, an iterative procedure is necessary to resolve the equilibrium equation. The resistance factors are taken as $\phi_{frp} = 0.80$ for the composite, $\phi_s = 0.85$ for steel, and $\phi_c = 0.85$ for concrete.

Calculations show that the neutral axis position for the Sainte-Émélie bridge T-beams falls in the slab, and the effective width b used in the calculations is the distance between parallel beams, measured centre to centre. The factored resisting moment can then be computed as

$$[6] \quad M_r = \phi_s f_y A_s \left(d - \frac{a}{2} \right) + \phi_{frp} E_{frp} A_{frp} \varepsilon_{frp} \left(h - \frac{a}{2} \right)$$

where d is the distance to the steel reinforcement, measured from the top of the beam, and h is the height of the section. The tensile forces in the section are shared between the steel reinforcement of area A_s and FRP longitudinal reinforcement A_{frp} .

For shear, the method used for calculating the amount of FRP stirrups required was also adapted from the simplified method for reinforced concrete sections that can be found in CSA Standard S6-1988. The shear strength of the section will be given by the sum of each material contribution, that is,

$$[7] \quad V_r = \phi(V_c + V_s) + V_{frp}$$

where V_{frp} , the shear strength of the external FRP stirrups, was added to the original equation. In this equation, the concrete shear strength is

$$[8] \quad V_c = v_b b_w d$$

and the contribution of the steel stirrups is given by

$$[9] \quad V_s = \frac{A_v f_y d}{s}$$

A method for calculating the value of v_b is prescribed in the S6 standard. Other values in the above equations are the web width b_w , height of the section d , and spacing of the internal stirrups s . The resistance factor is taken as $\phi = 0.75$.

It was estimated that the external FRP stirrups would provide the following shear strength:

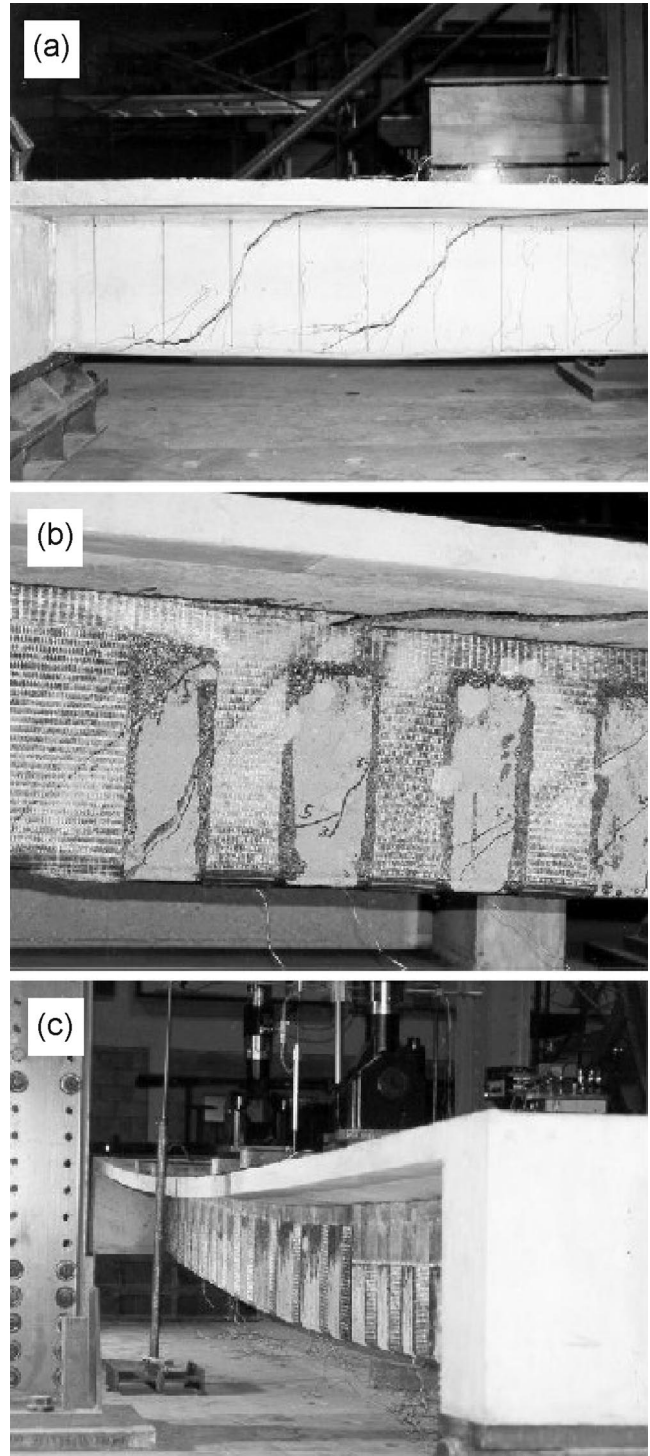
$$[10] \quad V_{frp} = \frac{\phi_{frp} A_{frp} E_{frp} \varepsilon_{frpe} d_{frp}}{s_{frp}}$$

with

$$[11] \quad A_{frp} = 2w_{frp} t_{frp}$$

where w_{frp} is the width of one stirrup of thickness $t_{frp} = 1.0$ mm, with spacing s_{frp} measured centre to centre. For the beams considered, the effective depth of the FRP stirrups was taken as $d_{frp} = 1257$ mm, their effective maximum strain was estimated at $\varepsilon_{frpe} = 0.0035$, and the value of the resistance factor ϕ_{frp} was chosen to be 0.75.

Fig. 7. Failure modes of 1:3 scale T-beams: (a) beam T1; (b) beam T2; and (c) beam T3.



6.2. Design options

Two design options were proposed to reinforce the Sainte-Émélie bridge (Demers et al. 1998) and were included in the Request for Proposals. The two cases differ only in CFRP type, this product being commercially available in the shape of sheets or strips; the amount of carbon fibres in the reinforcement was approximately the same for the two design

Fig. 8. FRP reinforcement for the Sainte-Émélie bridge.

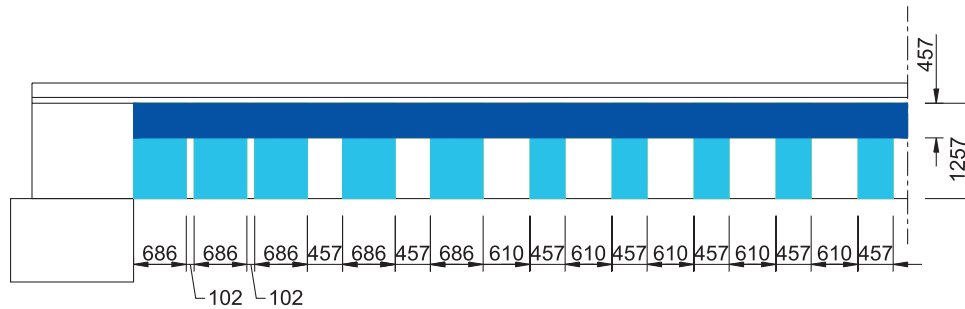


Fig. 9. Moment envelope for FRP-strengthened beams.

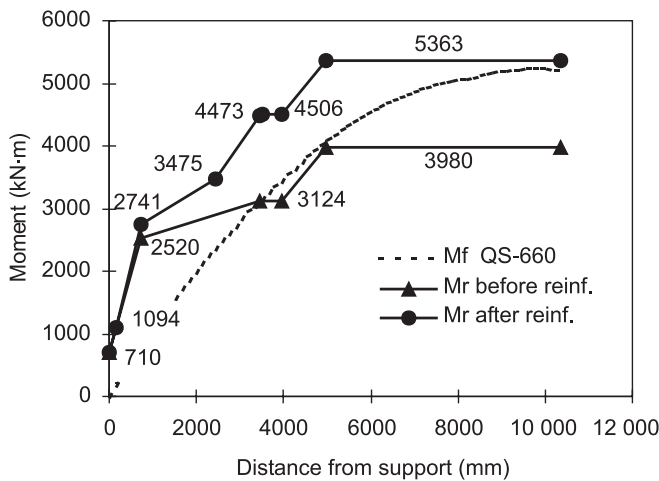
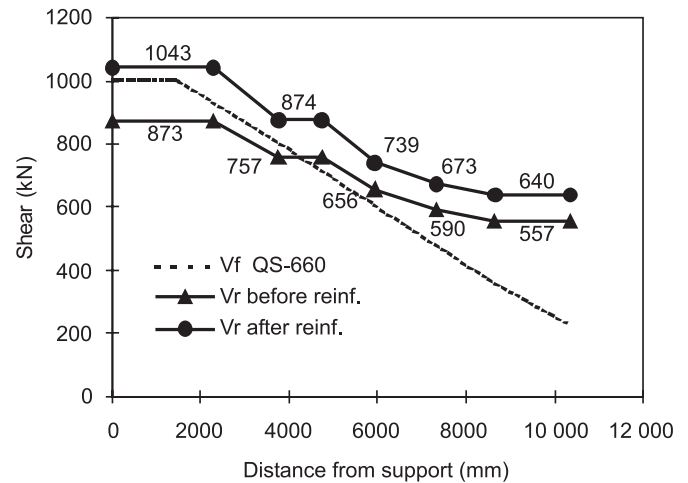


Fig. 10. Shear envelope for FRP-strengthened beams.



options. The FRP reinforcement prescribed for the four beams was identical. The option that was selected by the contractor is the one shown in Fig. 8. Bending reinforcement was to be provided by three longitudinal strips of Sika Carbodur S1214, which is a carbon-reinforced product 120 mm in width. Calculation for the bending strength of the section was done with $f_{frp} = f_u = 2400$ MPa, $E_{frp} = 155\ 000$ MPa, and a thickness of 1.4 mm. The three strips were to be installed on the full length of the beam; it was estimated that the anchorage would be sufficient, and that stirrups would not be required to prevent debonding of these strips. Due to material availability, the proposed reinforcement was replaced on site by six 60-mm-wide Carbodur strips with the same thickness and mechanical properties.

For shear reinforcement, the Request for Proposals specified glass-FRP, and Sikawrap Hex 100G was selected for that purpose. The U-shaped stirrups are wrapped around the section, with fibres in the vertical direction, thus locally covering the longitudinal carbon-FRP reinforcement in the process. In the central area of the beams, the 457-mm-wide layers of GFRP are separated by 610-mm-wide sections of unreinforced concrete. Figure 8 shows how the spacing of the stirrups is reduced near the beam supports and how the width of the stirrups simultaneously increases to 686 mm.

The total quantity of composites installed on the bridge amounts to 490 linear metres of Carbodur strips and 210 square metres of Sikawrap Hex 100G. While the beam strengthening was designed using the simplified methods described above, a more detailed analysis was also performed.

This analysis was adapted from the general method proposed for conventional reinforced sections and takes into account local effects caused by the partial termination of the steel reinforcement. The bending moment envelope for the FRP-strengthened beam is provided in Fig. 9 and is compared to the load requirement. The envelope for the original beam is also shown in the same figure. The shear envelopes for the original and FRP-strengthened beams are provided in Fig. 10.

6.3. Repair work

The repair work took place in the fall of 1998. The bridge remained opened to traffic during the repair period, but the lanes under which the FRP was being installed were closed in alternation. The traffic lanes were thus closed for approximately one week each. The preparation of the concrete surfaces to receive the FRP strengthening turned out to be more difficult to achieve than anticipated. For instance, the amount of sandblasting to smoothen the concrete surface had been underestimated. The installation of the longitudinal carbon-FRP strips was completed in the estimated time, despite the use of twice the amount of linear reinforcement caused by the replacement of 120-mm-wide strips by 60-mm strips. Figure 11a shows the installation of a typical Carbodur strip under one of the concrete beams. Transverse U-shaped reinforcement turned out to be more problematic to put in place than expected. The sheets were difficult to manipulate because of their large size and heavy weight once impregnated with epoxy. A technique to impregnate the proper amount of

epoxy had to be devised on site to facilitate manipulation of the sheets and to avoid potential slippage of the stirrups on the concrete surface. There were practical difficulties in evacuating trapped air between the FRP and concrete, especially near the corners of the beams. Eventually, epoxy was injected under the hardened surface to fill up the voids that had not been mechanically removed at installation. Figure 11*b* illustrates the installation of FRP stirrups on the side of a beam. The appearance of a beam strengthened with longitudinal and shear FRP reinforcements is shown in Fig. 11*c*, where the superposition of the glass-FRP stirrups over the longitudinal carbon-FRP strips is clearly visible. A protective layer of paint was applied later to the strengthened beams. Since the repair took place in early fall, it was necessary to enclose the construction site and to heat the beams to ensure complete curing of the epoxy.

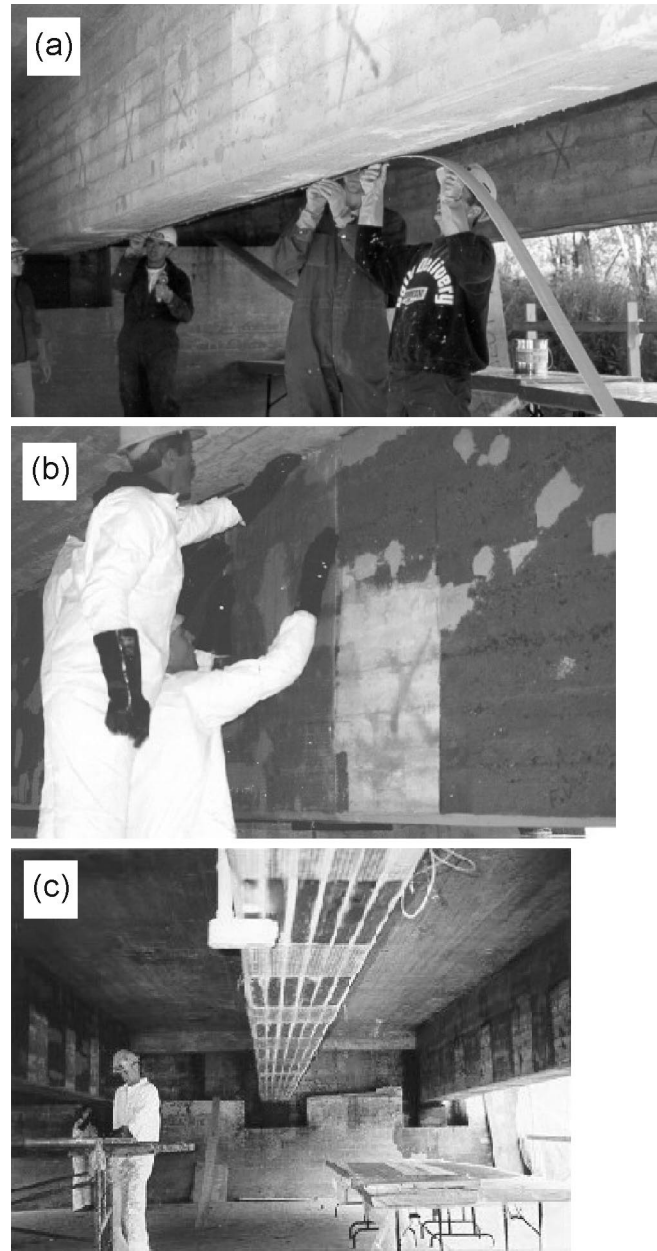
7. Instrumentation

To evaluate the structural efficiency of the FRP strengthening, the Sainte-Émélie bridge was instrumented with conventional resistive strain gauges. The mobile testing laboratory team of the MTQ installed eight gauges prior to the reinforcement. Concrete cover was removed around longitudinal rebars to allow installation of these strain gauges. They are all located at midspan of the bridge. Twenty additional gauges were installed by the Université de Sherbrooke research group upon completion of bridge strengthening, some of them at midspan and the others near the bridge supports. Midspan gauges are located either on the longitudinal FRP strips or on the side face of the section near the slab. Combination of data from the various gauges at a given location then allows a comparison of its strain profile under load with the design hypotheses. Although it can be expected that the loads near beam extremities will not be critical in bending, a number of strain gauges regularly spaced longitudinally in this area are expected to provide useful information on the shear transfer between concrete and FRP.

The integration of innovative sensors for continuous structural monitoring was an additional goal pursued by the research team. It was decided, at the planning stages of the Sainte-Émélie bridge strengthening, to incorporate sensors based on fibre optic technology into the structural reinforcement. Once attached to the structural element to be evaluated, these sensors contract or expand according to the variations in strain and temperature. The state of deformation is interpreted by measuring changes in the properties of the light that is reflected by the fibre optic sensors. The characteristics and working principles of the two types of devices incorporated in this bridge, which are either Fabry-Perot or Bragg Grating sensors, are described elsewhere (Tennyson et al. 2000). To compare strain measurements between conventional gauges and optic fibre sensors, the two systems were systematically installed near each other.

Table 3 provides a complete listing of the bridge instrumentation and location; it can be observed that, in addition to the strain gauges and optic fibre sensors, ten thermocouples were installed permanently to help correct potential errors due to temperature effects. Other instruments used during the tests included two load cells per beam to measure strains at midspan and one displacement sensor under each

Fig. 11. Strengthening of the bridge: (a) installation of longitudinal reinforcement; (b) installation of shear reinforcement; and (c) completion of beam strengthening.



beam. Accelerometers were also used for a number of dynamic tests.

8. Bridge testing

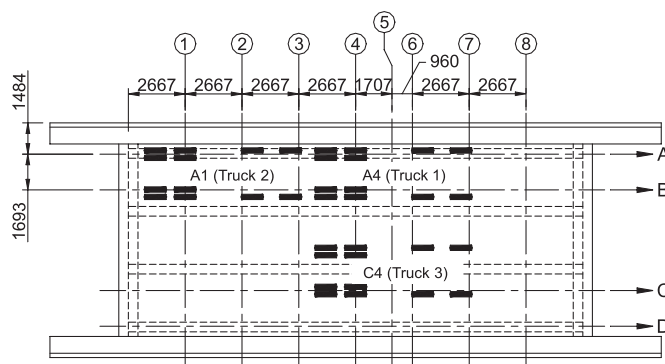
Loading tests were performed on the bridge under the direction of the Ministère des Transports du Québec. Three four-axle trucks of 33 tonnes were used to apply simulated traffic loading to the structure; identical loading sequences were imposed on the bridge before and after the FRP strengthening. Static and dynamic loading tests were performed (Labossière et al. 1999).

A typical location for the trucks during the static tests is shown in Fig. 12. Four different loading paths are identified

Table 3. Bridge instrumentation.

		West end		Midspan		East end	
		Exterior beams	Interior beams	Exterior beams	Interior beams	Exterior beams	Interior beams
Strain gauges	Steel rebars	—	—	4	4	—	—
	FRP	4	4	2	2	2	2
	Top of beam	—	—	2	2	—	—
Fabry-Perot gauges	Steel rebars	—	—	1	1	—	—
	FRP	—	4	1	1	—	—
Braggs gauges	Steel rebars	—	—	2	2	—	—
	FRP	4	—	2	2	2	2
	Top of beam	—	—	2	2	—	—
Thermocouples	Steel rebars	—	—	2	2	—	—
	FRP	1	1	2	—	1	1

Fig. 12. Loading paths on tested bridge.



as axes A to D on the bridge plan view. It will be noted that for A and D, the outer wheels of the truck are positioned over an exterior beam. For loading paths B and C, the centre of gravity of the truck is positioned over an interior beam. As it crosses the bridge from the west to the east, the truck stops at eight positions for the reading measurements. The bridge was loaded with a single truck in each of the four paths, then with combinations of two or three trucks. Table 4 provides a complete listing of the loading combinations for which measurements were obtained. For the dynamic load tests, the three trucks were successively driven across the bridge at moderate speed and requested to brake at midspan.

Only a limited selection of the results obtained during the two loading sessions is presented here. Since additional loading of the bridge will take place in the future, a more detailed analysis of the results will be presented in due course and will include time effects and durability considerations. However, a number of observations on the bridge strengthening and monitoring systems can already be noted.

The effects of loading case BC involving two trucks are particularly relevant, since this condition is the only one that is transversely symmetrical. The two trucks running in parallel were requested to stop with their third axle over positions 1 to 8. Figure 13 shows strain measurements obtained at midspan for the two interior beams of the bridge, with the trucks in the successive positions indicated on the horizontal axis. These measurements were taken before FRP strengthening. One of the interior beams was instrumented with re-

sistive gauges J121 and J122, while the other one was instrumented with gauges J131 and J132. The two resistive gauges on each beam provided basically the same results, and it can be observed that the measurements in the two beams were almost similar for all stopping positions. The difference between gauges never exceeds 3% under identical loading conditions. Maximum strains were measured when the centre of gravity of the loads coincided with the centre of the bridge. In addition to the resistive gauge measurements, Fig. 13 indicates the strains that were measured by Bragg fibre optic sensors B17 and B20 at the same locations. It can be observed that these values are consistently lower than those measured by the resistive gauges, by a factor of about 30%. Excessive sensitivity of the fibre optic demodulating system to changes in temperature appears to be the main reason to explain this difference. However, this problem is still being investigated.

When the load applied to the bridge with three trucks is not symmetrical with respect to the bridge axis, such as loading paths ACA and DBD, they are expected to produce anti-symmetrical results with respect to each other. This is shown in Fig. 14 where the strain measurements obtained for the two cases are presented. Strain gauges J111 and J112, located on one side beam, should be submitted under loading path ACA to the same strains as gauges J141 and J142 under loading path DBD. It can be observed that the two resistive gauges located on a given beam provided identical results. The maximum strain is found in the two beams for the same relative position of the trucks, that is, A6C6A2 in one case and D6B6D2 in the second case. The difference of 12% between the maximum strains measured in the two beams appears reasonable in view of the bridge and truck characteristics. For instance, site measurements have indicated that the position of the steel rebars is not exactly at the same height in the two beams. In addition, the load of the three trucks was not exactly identical. The figure shows differences of the same order of magnitude between the fibre optic sensors B14 and B23 at similar locations.

The effect of bridge strengthening at a specific location is shown in Fig. 15 for loading path ACA, that is, with two vehicles in lane A and one in lane C. In this case, the two front trucks are running parallel to each other in lanes A and C, followed by the third one also in lane A. At the first point of measurement, A4C4, the third axles of the two front trucks

Table 4. Loading paths.

Path	Stop position									
	0	1	2	3	4	5	6	7	8	End
A	A0	A1	A2	A3	A4	A5	A6	A7	A8	A
B	B0	B1	B2	B3	B4	B5	B6	B7	B8	B
C	C0	C1	C2	C3	C4	C5	C6	C7	C8	C
D	D0	D1	D2	D3	D4	D5	D6	D7	D8	D
BC	BC0	B1C1	B2C2	B3C3	B4C4	B5C5	B6C6	B7C7	B8C8	BC
ACA	ACA0	A4C4	A4C4A1	A6C6A2	A7C7A3	A8C8A4	A5	A6	A7	ACA
DBD	DBD0	D4B4	D4B4D1	D6B6D2	D7B7D3	D8B8D4	D5	D6	D7	DBD

Fig. 13. Results for loading path BC: (a) beam 2 and (b) beam 3.

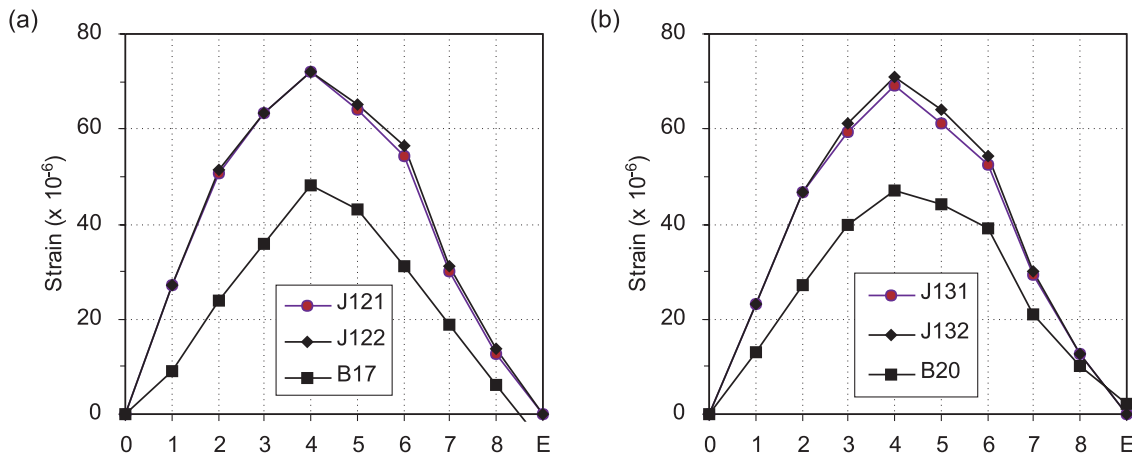
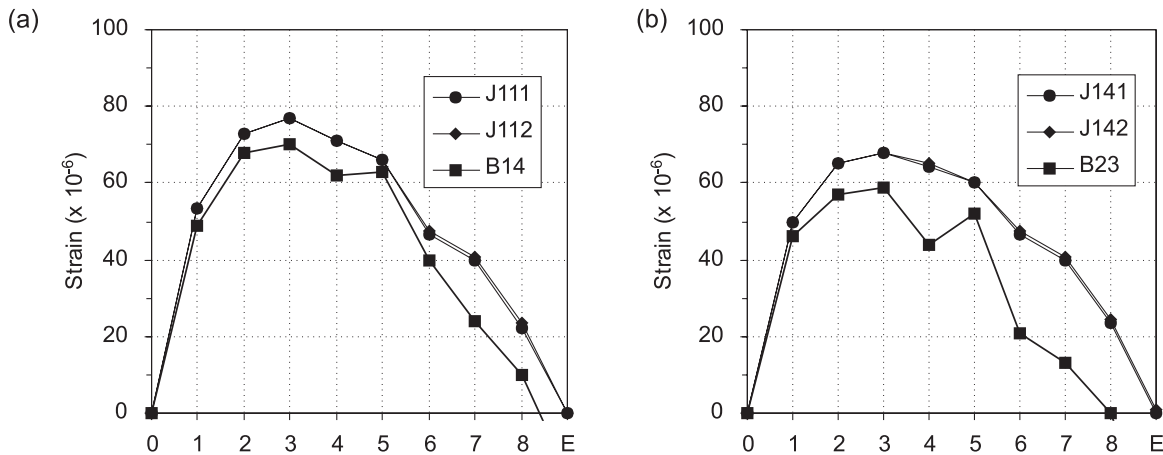


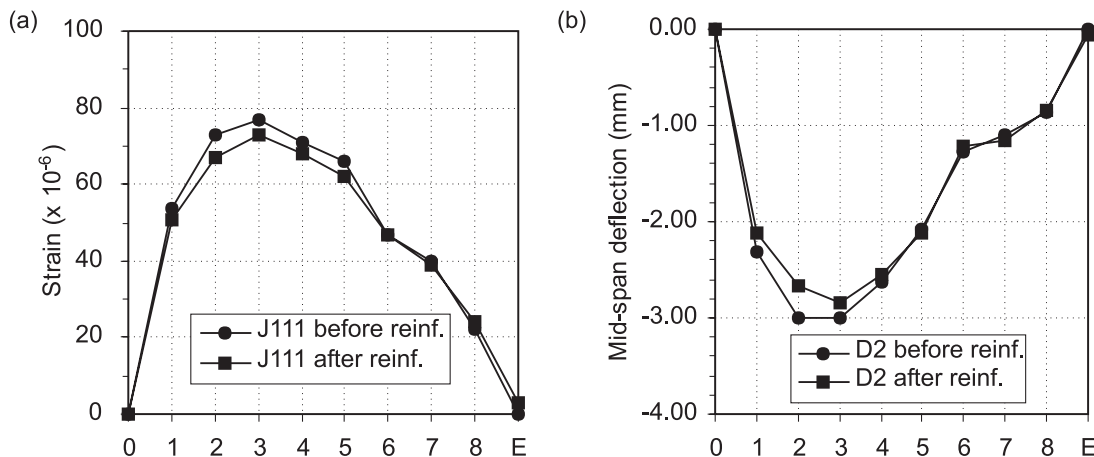
Fig. 14. Comparison of loading paths: (a) effect of path ACA on beam 1 and (b) effect of path DBD on beam 4.



are stopped over line 4; for the second measurement, a third truck was positioned with its third axle over line 1, and the loading case was identified as A4C4A1. The eight loading cases are identified on the horizontal axis of the figure. The left-hand-side figure provides the measured strain in the resistive gauge J111 installed on a steel rebar at midspan of a side beam, while the right-hand-side figure provides the midspan deflection as measured from the displacement sensors. The data obtained before strengthening can be compared to the post-reinforcement measurements. At midspan, maximum strains and displacements were obtained for the

loading case A6C6A2. There is an excellent correlation between the two sides of the figure, the deflection being inversely proportional to the maximum strain. This relationship is maintained before and after reinforcement. For the loading case with the maximum effect, the increase in stiffness of the section is about 5%. Considering the small size of the additional reinforcement, this measured increase is compatible with the design expectations.

Strain measurements have been taken on an intermittent but regular basis since the FRP strengthening was installed on the bridge. Up to this point, measurements do not indi-

Fig. 15. Effect of loading path ACA before and after strengthening: (a) beam 1 and (b) beam 2.**Table 5.** Construction schedule.

Activity	Date
Site preparation, platform installation	Sept. 8–9
Installation of gauges on existing steel reinforcement	Sept. 10–11
Loading test	Sept. 14
Repair of concrete (sandblasting, mortar)	Sept. 15 – Oct. 2
FRP, westbound side: flexural	Sept. 28–29
FRP, westbound side: shear	Sept. 30 – Oct. 1
FRP, eastbound side: flexural	Oct. 6–7
FRP, eastbound side: shear	Oct. 7–8
Installation of fibre optic sensors on strengthened structure	Oct. 8–13
Loading test	Oct. 14
Completion of repair work	Oct. 16

cate any significant strain changes since the repair took place. However, other sessions of truck loading are planned in the future to evaluate the durability of the repair work. In addition, data from the fibre optic sensors will be obtained continuously over weekly periods to evaluate their usability as a monitoring device.

9. Schedule and cost issues

In the summer of 1998, the Ministère des Transports du Québec issued the drawings and official documents for a limited Request for Proposals. Submissions were invited only from companies with previous experience in the repair and strengthening of structures with FRPs, or having a proven record of high work quality. The contract was awarded for \$97 950, compared to a previous estimate of \$96 000 from the MTQ. It was found on site that the extent of the concrete repair had been underestimated. Minor repairs on the abutments were also requested from the contractor. In addition, it was found that the installation of a protective coating over the FRP had been omitted from the Call for Tenders. All these changes led to a total construction cost of \$108 500. According to the MTQ, this would compare to 50% of the total cost for the replacement of the

infrastructure. This kind of repair would be viewed as economically viable if it could be lowered to approximately 33% of the replacement. It is obvious in this case that special attention to detailing and extra time spent on the construction to take into account a number of research objectives were sources of additional costs, which would not be incurred in another similar project.

Construction began on the Sainte-Émélie strengthening project on September 8, 1998, and the post-strengthening tests were completed approximately 6 weeks later, on October 16. Table 5 provides a general schedule of the construction and testing activities on the Sainte-Émélie bridge. It can be noted that the actual repair-related activities, including site preparation, surface cleaning, and installation of the FRP strengthening, were completed in 21 working days. During this period, the only inconvenience to the user was the alternative closing of one lane for the 8 working days necessary to install the composite materials.

10. Conclusions

The strengthening of the Sainte-Émélie-de-l'Énergie bridge with FRP was the first project of this magnitude under the responsibility of the MTQ. The design of the reinforcement was carried out after an evaluation of the strengthening technique in a series of 1:3 scale tests performed at the Université de Sherbrooke. The reinforcement was originally designed to provide a 35% increase in bending capacity and 20% in shear strength to this structure, which was built in 1951. The installation of the composites was achieved efficiently, despite the fact that the degradation of the concrete surface was more severe than first anticipated. In fact, most difficulties observed on the construction site were related to the condition of the original structure. The instrumentation incorporated into the bridge includes conventional resistive strain gauges and innovative fibre optic sensors. The loading tests performed on the bridge have confirmed that its behaviour is consistent with the design hypotheses for the FRP reinforcement. Additional measurements are planned in the future.

Acknowledgements

This research project was supported by the Natural Sciences and Engineering Research Council of Canada (NSERC) through the Network of Centres of Excellence (NCE) ISIS Canada; this support is gratefully acknowledged. Additional funding for the laboratory testing was granted by the Ministère des Transports du Québec, owner of the Sainte-Émélie bridge. The technical assistance of Claude Aubé, Yves Beaudoin, and Laurent Thibodeau was essential in the completion of the laboratory setup. The authors also wish to acknowledge the collaboration of the MTQ mobile laboratory team led by Dr. Marc Savard for the bridge loading tests and acquisition of data.

References

- CSA. 1988. Design of highway bridges. Standard S6-88, Canadian Standards Association, Toronto, Ont.
- Demers, M., Lapierre, P., and Lamothe, P. 1998. Renforcement de poutres de pont en travée simple avec des matériaux composites — Phase II : Détails du renforcement avec des matériaux composites du pont en béton armé #03284 et notes de calcul — Sainte-Émélie-de-l'Énergie. Report ISIS 98-101-201, presented to Ministère des Transports du Québec, Sherbrooke, Que.
- Japan Concrete Institute. 1997. Non-metallic (FRP) reinforcement for concrete structures. Proceedings of the Third International Symposium on Non-Metallic (FRP) Reinforcement for Concrete Structures, Vols. 1 and 2, Sapporo, Japan.
- Labossière, P., Beaudoin, Y., Lamothe, P., Lapierre, P., Neale, K.W., Demers, M., and Martel, S. 1998. Renforcement de poutres de ponts en travée simple avec des matériaux composites : Projet de recherche — Phase I. Report ISIS 98-101-101, presented to Ministère des Transports du Québec, Sherbrooke, Que.
- Labossière, P., Demers, M., Rochette, P., and Neale, K.W. 1999. Renforcement de poutres de ponts en travée simple avec des matériaux composites : Projet de recherche — Phase II. Report ISIS 99-101-101, presented to Ministère des Transports du Québec, Sherbrooke, Que.
- Lamothe, P., Labossière, P., and Neale, K.W. 1998. Post-strengthening of reinforced concrete T-beams with composite materials. Proceedings of the Canadian Society for Civil Engineering Annual Conference, Halifax, N.S. *Edited by* J.P. Newhook and L.G. Jaeger. pp. 623–631.
- Lapierre, P., Labossière, P., and Neale, K.W. 1998. Modélisation de poutres en T en béton armé renforcées avec des matériaux composites. Proceedings of the Canadian Society for Civil Engineering Annual Conference, Halifax, N.S. *Edited by* J.P. Newhook and L.G. Jaeger. pp. 613–622.
- Meier, U., and Betti, R. 1997. Recent advances in bridge engineering: evaluation, management and repair. Proceedings of the U.S.–Canada–Europe Workshop on Bridge Engineering, Zurich, Switzerland.
- Neale, K.W., and Labossière, P. 1998. Fiber composite sheets in cold climate rehab. *ACI Concrete International*, **20**(6): 22–24.
- Ministère des Transports du Québec. 1994. Ouvrages d'art : normes Tome III de Ouvrages routiers. Publications du Québec, Sainte-Foy, Que.
- Rizkalla, S.H., and Labossière, P. 1999. FRP in structural engineering in Canada: planning for a new generation of infrastructure. *ACI Concrete International*, **21**(10): 25–28.
- Tennyson, R.C., Coroy, T., Duck, G., Manuelpillai, G., Mulvihill, P., Cooper, D.J.F., Smith, P.W.E., Mufti, A.A., and Jalali, S.J. 2000. Fibre optic sensors in civil engineering structures. *Canadian Journal of Civil Engineering*, **27**(5): 880–889.